Cancer Immunology, Immunotherapy (2025) 74:135
https://doi.org/10.1007/s00262-025-03989-2

RESEARCH

LPIN3 promotes colorectal cancer growth by dampening intratumoral CD8$^+$ T cell effector function

Xiaoming Zhang[1] · Hao Fang[2] · Wenliang Wu[3] · Congqing Jiang[1] · Haizhou Wang[4] · Yifei Shi[5]

Received: 16 December 2024 / Accepted: 19 February 2025

Abstract

LPIN3 has emerged as a key factor in a variety of malignancies, although its precise role in colorectal cancer (CRC) remains unclear. By analyzing the data from The Cancer Genome Atlas, we discovered that the expression pattern of LPIN3 and the relevant makeup of the immune microenvironment were immensely diverse among tumors. LPIN3 is abundantly expressed in CRC and may enhance tumor growth by activating the β-catenin signaling pathway. In addition, we discovered that LPIN3 might reduce tumor antigen presentation signals, hence suppressing CD8$^+$ T cell-mediated cytotoxicity. Furthermore, high expression of LPIN3 predicts decreased CD8$^+$ T cell infiltration and effector function via bioinformatics analysis. Indeed, CD8$^+$ T cell-mediated cytotoxicity as well as CD8$^+$ T cell infiltration and activation in vivo were strengthened by LPIN3 knockdown. To sum up, our results highlight the part that LPIN3 plays in driving the progression of CRC by regulating β-catenin signaling and CD8$^+$ T cell activity.

Keywords Colorectal cancer · LPIN3 · Immune evasion · Immunotherapy

Introduction

Colorectal cancer (CRC) is a common tumor in the digestive system, with 2.5 million new cases worldwide predicted by 2035 [1]. Despite the treatment progress, such as immunotherapy, CRC mortality rate ranks third among deaths caused by tumors [2]. Therefore, understanding the molecular mechanisms underlying its development and progression is of paramount importance.

LPIN3 (Lipin 3) is an enzyme that belongs to the Lipin family (also includes Lipin-1 and Lipin-2), involving in lipid metabolism [3]. These proteins play crucial roles in the synthesis of triglycerides and phospholipids by converting phosphatidic acid (PA) to diacylglycerol (DAG) which is an essential step in lipid metabolism. Lipin proteins also function as transcriptional coactivators, influencing the expression of genes that involved in lipid metabolism [4]. LPIN3 is expressed notably in the small intestine, where it plays a role in lipid absorption, and in other tissues related to lipid processing, such as the liver, kidneys, and gastrointestinal tract [5].

Given such an important physiological function of LPIN3, however, its role in the process of tumor development has been little studied. Only a few bioinformatics analyses have shown that LPIN3 can be used as a risk

Xiaoming Zhang, Hao Fang and Wenliang Wu have contributed equally.

✉ Congqing Jiang
wb002554@whu.edu.cn

✉ Haizhou Wang
2016203030002@whu.edu.cn

✉ Yifei Shi
11918416@zju.edu.cn

1 Department of Colorectal and Anal Surgery, Zhongnan Hospital of Wuhan University, Wuhan 430071, China

2 Department of Gastroenterology, Ningbo No.2 Hospital, Ningbo 315010, China

3 Division of Gastrointestinal Surgery, Department of Surgery, Wuhan No.1 Hospital, Wuhan 430022, China

4 Department of Gastroenterology, Zhongnan Hospital of Wuhan University, Wuhan 430071, China

5 Department of Radiology, The Second Affiliated Hospital, Zhejiang University School of Medicine, Hangzhou 310009, China

Published online: 05 March 2025

predictor in tumors such as prostate [6], ovarian cancers [7, 8] and hepatic lipid metabolism [9], but there have been no experiments to investigate its role in tumor progression, especially in colorectal cancers, where it is predominantly expressed. Therefore, the role of LPIN3 in regulation of the important signaling cascades that associated with carcinogenesis needed to be deeply explored.

Cancer immunotherapy has completely changed the treatment strategies, which are treated by specifically targeting the immune system and resulting in the elimination of tumors [10]. Nonetheless, tumor immune evasion continues to pose a serious obstacle, decreasing the efficacy of immunotherapy. Strategies that avoid immune system recognition and elimination, including the upregulation of immune checkpoint molecules [11], such as cytotoxic T-lymphocyte-associated protein 4 (CTLA-4) and programmed cell death protein 1 (PD-1) were adopted by cancer cells to escape the immunotherapy [12]. Tumor can block T cell activation and decrease the major histocompatibility complex (MHC) molecules [13, 14] that are essential for presenting tumor antigens to T cells. Tumors can also attract immune-suppressive cells, such as myeloid-derived suppressor cells (MDSCs) [15] and regulatory T cells (Tregs), which together provide an immunosuppressive milieu that promote immune evasion and tumor growth.

Comprehending the complex correlation between LPIN3 and tumor immune evasion might potentially lead to the creation of innovative immunotherapeutic approaches, aiming at surmounting this crucial obstacle to successful cancer therapy. Targeting LPIN3 and its downstream signaling pathways may restore the immune cell function, strengthen the antitumor immune response, and increase the effectiveness of current immunotherapies. Furthermore, LPIN3 may be a useful indicator for predicting immunotherapy response and directing cancer patients' treatment choices.

Methods

Data extraction and data processing

In relation to The Cancer Genome Atlas (TCGA-COAD) data, the TCGA website (www.cancer.gov/tcga) included RNA sequencing transcriptome data for 514 samples of patients with colorectal cancer (CRC), which included 473 cancer specimens and 41 specimens from normal tissues. The data were also accompanied by clinical pathology information. GSE35279 was obtained from The Gene Expression Omnibus (GEO) database, which contained 74 CRC samples and five normal samples. All the data were transformed into $\log_2$ (TPM + 1).

Cell culture

The mouse CRC cell CT26, the human CRC cells HCT116 and RKO, and the human embryonic kidney epithelial cell HEK-293T were procured from the National Infrastructure of Cell Line Resource and maintained in Dulbecco's Modified Eagle Medium (DMEM) supplemented with 10% fetal bovine serum (FBS) and 1% penicillin G/streptomycin. Cells were incubated at 37 °C in a humidified atmosphere with 5% CO_2.

Short hairpin RNA (shRNA) and vector construction

A shRNA fragment targeting the CDS or UTR of human LPIN3 was generated using a pair of primers (forward primer1: 5′-CCGGGAGCTCATAAAGAACCACAA ACTC GAGTTTGTGGTTCTTTATGAGCTCTTTTTG -3′; forward primer2: 5′-CCGGCCA CTGTCTTTGAAG AAAGTACTCGAGTACTTTCTTCAAAGACAGTGG TTTTTG-3′); of mouse Lpin3 was generated using a pair of primers (forward primer1: 5′-CCGGCCCAGAGAGTA AGGAAACCAACTCGAGTTGGTTTCCTTACTCTC TGGGTTTTTG-3′; forward primer2: CCGGCCTAAGAG TGACTCAGAGCTACTCG AGTAGCTCTGAGTCACTC TTAGGTTTTTG) and cloned into the plasmid pLKO.1-TRC (Addgene) as described in the TRC protocols (http://www.broadinstitute.org).

Lentiviral transduction of tumor cells

Lentivirus-induced LPIN3 knockdown in CT26, HCT116, and RKO cells was performed as following steps: 4 μg PLKO.1 plasmid of shCtrl or shLPIN3, 3 μg psPAX2 packaging vector, and 1 μg PMG2.G enveloping vector were co-transfected into HEK-293 T cells in 10-cm cell-culture dishes. The virus-containing supernatant was collected after 48 and 72 h, filtered using a 0.45 μm PES Syringe Filter (Thermo Fisher), and utilized to infect tumor cells in the presence of 8 mg/ml Polybrene. After selecting the positive infected cells for 7 days using 2 μg/ml puromycin (Solarbio) for specified cells, stable cell lines were subsequently maintained under puromycin.

Western bolt

1 ml of cell lysis buffer (50 ml tris-base (pH 7.4), 150 ml sodium chloride, 1% Nonidet P-40, 0.5% sodium deoxycholate, 0.1% sodium dodecyl sulfate, 5 ml ethylene diamine tetraacetic acid (EDTA), and 1 ml benzylsulfonyl fluoride) was utilized to lyse transfected cells. As

previously indicated, immunoblot analysis was performed [16].

Flow cytometry

The tumor tissues from shCtrl or shLpin3 CT26 were digested for 30 min at 37 °C with 1 mg/ml Collagenase D and 0.1 mg/ml DNase I (Solarbio). After stopping the digestion with EDTA, the cells were filtered through 70 μm cell strainers and twice washed with phosphate buffered saline (PBS) containing 2% FBS and 1 mM EDTA (staining buffer). After resuspension in the staining solution, the following antibodies were applied to the cells for 30 min on ice: anti-CD8, anti-IFN-γ, anti-PD-1, anti-TOX, anti-TNF-α, and anti-Granzyme B (GZMB) (all from BioLegend) [17]. Gating strategies for flow cytometry analysis are provided in Figure S6.

Cell proliferation assay

For CCK-8 experiments, 1×10^3 cells were seeded in 96-well plates per well, and incubated five days. And 10 ul Cell-Counting-Kit-8 reagent (Vazyme, China) was added in per well, which was incubated at 37 °C for 1 h. The absorption was evaluated by measuring the absorbance at 450 nm in accordance with the manufacturer's instructions.

Transwell assay

For the cell invasion assay, 5×10^4 CRC cells suspended in 200 μL were seeded into the upper chamber pre-coated with Matrigel, while the lower chamber contained culture medium supplemented with 20% FBS as a chemoattractant. After 48 h of incubation, non-invading cells on the upper surface of the membrane were removed. The invading cells on the underside of the membrane were then fixed, stained with 0.1% crystal violet, and subsequently observed and counted under a microscope.

Colony formation assay

For the colony formation assay, 2×10^3 CRC cells were seeded in six-well plates and cultured for 14 days. After incubation, the colonies were fixed with paraformaldehyde and stained with 0.1% crystal violet. The plates were then washed with PBS, and colonies consisting of more than 50 cells were counted and photographed.

Scratch wound healing assay

CRC cells were seeded into 6-well plates and cultured overnight to reach approximately 90% confluence in a monolayer. A scratch wound was then created across the center of each well using a 200-μL pipette tip. Subsequently, the culture medium was replaced with one containing 1% FBS. Wound closure was assessed, and images were captured under a microscope at 0 and 48 h. The healing area was quantified using ImageJ software.

Cell apoptosis assay

Prior to starting the experiments, a 24-well plate was seeded with 1×10^3 cancer cells. Cells were obtained by centrifugation at 300 g for 5 min at 4 °C following digestion with EDTA-free trypsin. Trypsin digestion was carefully regulated to minimize excessive time in order to prevent false positives. After that, the cells were centrifuged for five minutes at 4 °C after being cleaned twice at 300 g using pre-cooled PBS. After the PBS was removed, 100 μl of 1 × Binding Buffer was added to bring the cells back to suspension. Next, 5 μl of Annexin V-FITC was added, and it was gently mixed. The combination was exposed to light and left to react for ten to fifteen minutes at room temperature. Subsequently, 200 μl of 1 × Binding Buffer was introduced, combined, and chilled. Ultimately, within one hour, samples were detected using fluorescence microscopy or flow cytometry [18].

Pan-cancer expression analysis of LPIN3 and related immune infiltration analysis

The TIMER website (https://cistrome.shinyapps.io/timer/) and R package "TCGAplot" were used to analyze the LPIN3 expression among the 33 cancers. The TIMER website is a web server designed for in-depth analysis of tumor-infiltrating immune cells. Utilizing this database, researchers investigated the correlation between LPIN3 expression and various immune cell populations, including $CD8^+$ T cells, neutrophils, and macrophages et al. Immune signaling set analysis was performed by ssGSEA algorithm [19].

Mouse model and tumor studies

For the in vivo trials, male BALB/c or nude mice, aged eight weeks, were randomly divided groups and each group contained five mice. shCtrl and shLpin3 cells in the logarithmic growth phase were digested and resuspended in the PBS in a density of 1×10^7 cells per 1 ml. Next, a 100 μl cell solution was subcutaneously administered into the right flanks of mice. Mice were housed in identical conditions, and the tumor growth was monitored every three days. The tumor volume was calculated as follows: Volume = length × width^2 × 1/2.

Tumor-infiltrating CD8$^+$ T cell analysis

After the tumor tissue was cut into small pieces, it was put through an enzymatic digestion procedure using 200 µg/ml collagenase and 20 µg/ml DNase for 30 min at 37 °C. Following digestion, the tumor tissue suspension was filtered through a 0.45 µm filter, and the single-cell suspension that remained was collected. The obtained cells were treated with Golgiplug protein transport inhibitor according to the manufacturer's instructions. After that, the cells were stained with CD8 antibody, intracellular IFN-γ, and GZMB antibody for 30 min at 4 °C. Then, a flow cytometry study was performed using the BD X20 cytometer (BD Biosciences).

Statistical analysis

The mean ± SD is used to display the data. The Student's t test was employed to compare the two groups. The one-way ANOVA was employed to compare data among several groups. For all statistical studies, GraphPad Prism version 9.5 was used. For nonparametric data, the Wilcoxon test was used for comparisons of two independent samples, whereas the Kruskal–Wallis test was used for multiple sample comparisons. A difference that was deemed statistically significant was defined as $P < 0.05$, and p-values < 0.01 and < 0.001 were denoted by ** and ***, respectively.

Results

The expression pattern and prognosis of LPIN3 in pan-cancers

The differential expression and paired differential expression analysis of LPIN3 in multiple cancers were performed by TIMER2.0 (http://timer.cistrome.org/) and TCGA data, respectively. Both the results supported that the mRNA expression level of LPIN3 was upregulated in several cancer types compared with adjacent normal tissues, including the bladder urothelial carcinoma (BLCA), kidney's clear cell carcinoma (KIRC), head and neck squamous cell carcinoma (HNSC), liver hepatocellular carcinoma (LIHC), liver hepatocellular carcinoma (LUAD), liver hepatocellular carcinoma (LUSC), stomach adenocarcinoma (STAD), and colon adenocarcinoma (COAD) (Fig. 1A, B). Furthermore, the high expression level of LPIN3 was significantly correlated with the poor prognosis of patients with pancreatic cancer, ovarian cancer, and LIHC (Fig. 1C). These findings indicated that the upregulation of LPIN3 in variety of cancer types may play a crucial role in cancer progression.

Tumor immune infiltration, immune-related molecules analysis in pan-cancers based on the expression of LPIN3

In order to ascertain the immunological function role of LPIN3 in pan-cancers, the correlation between the expression of LPIN3 and the immune cell infiltration was examined. The ssGSEA analysis showed that LPIN3 was negatively associated with the immunological score (EstimateScore, ImmuneScore, StromalScore) in pan-cancers but the lymphoid neoplasm diffuse large B-cell lymphoma (DLBC), brain lower grade glioma (LGG) (Fig. 2A). And the expression level of LPIN3 was correlated with multiple immune-related inhibitory substances. The findings showed that in some cancer types, such as COAD and BLCA, LPIN3 was substantial negatively associated with the expression of many immune-related inhibitory molecules, including CD244, CTLA-4, TGFBR1, TIGIT, and IL10 (Figs. 2B and S1A). Additionally, it was shown that there was a strong positive correlation between LPIN3 and the expression of chemokines and chemokine receptors (Figure S1B). Additionally, LPIN3 was also tightly associated with the expression of several immunomodulatory molecules as well as various immunological checkpoints (Fig. 2C). These results suggested that there may be diametrically opposed effects of LPIN3 on the immune microenvironment in different tumor types.

LPIN3 promotes CRC growth in In vivo *and* in vitro

Due to the strong association between LPIN3 and immune microenvironment in COAD, we further adopted another independent cohort to investigate the expression pattern of LPIN3 in COAD. The expression level of LPIN3 was upregulated in tumor tissues compared with normal tissues in TCGA-COAD dataset (https://ualcan.path.uab.edu/) (Fig. 3A) and the GSE35579 cohort (Fig. 3B). Log-rank survival analysis based on OS, DSS, DFI, and PFI was carried out to precisely ascertain the relationship between LPIN3 expression and the prognosis of patients in TCGA-COAD cohort (Fig. 3C). The results showed that high expression of LPIN3 in CRC indicated a poor prognosis (Figure S2A–C). The expression of LPIN3 in different stages, histological subtypes, nodal metastasis status, and TP53 mutation status of CRC, was found to be considerably higher than those in normal tissues (Figure S2D–G). Human CRC cells HCT116 and RKO were subjected to shRNA-mediated LPIN3 knockdown to ascertain whether LPIN3 had an impact on CRC growth. The mRNA and protein level of LPIN3 was significantly reduced in HCT116 and RKO cells after knockdown (Fig. 3D–G). The results of the cell proliferation assay showed that the deficiency of LPIN3 substantially reduced the cell growth of HCT116 and RKO cells in vitro (Fig. 3H,

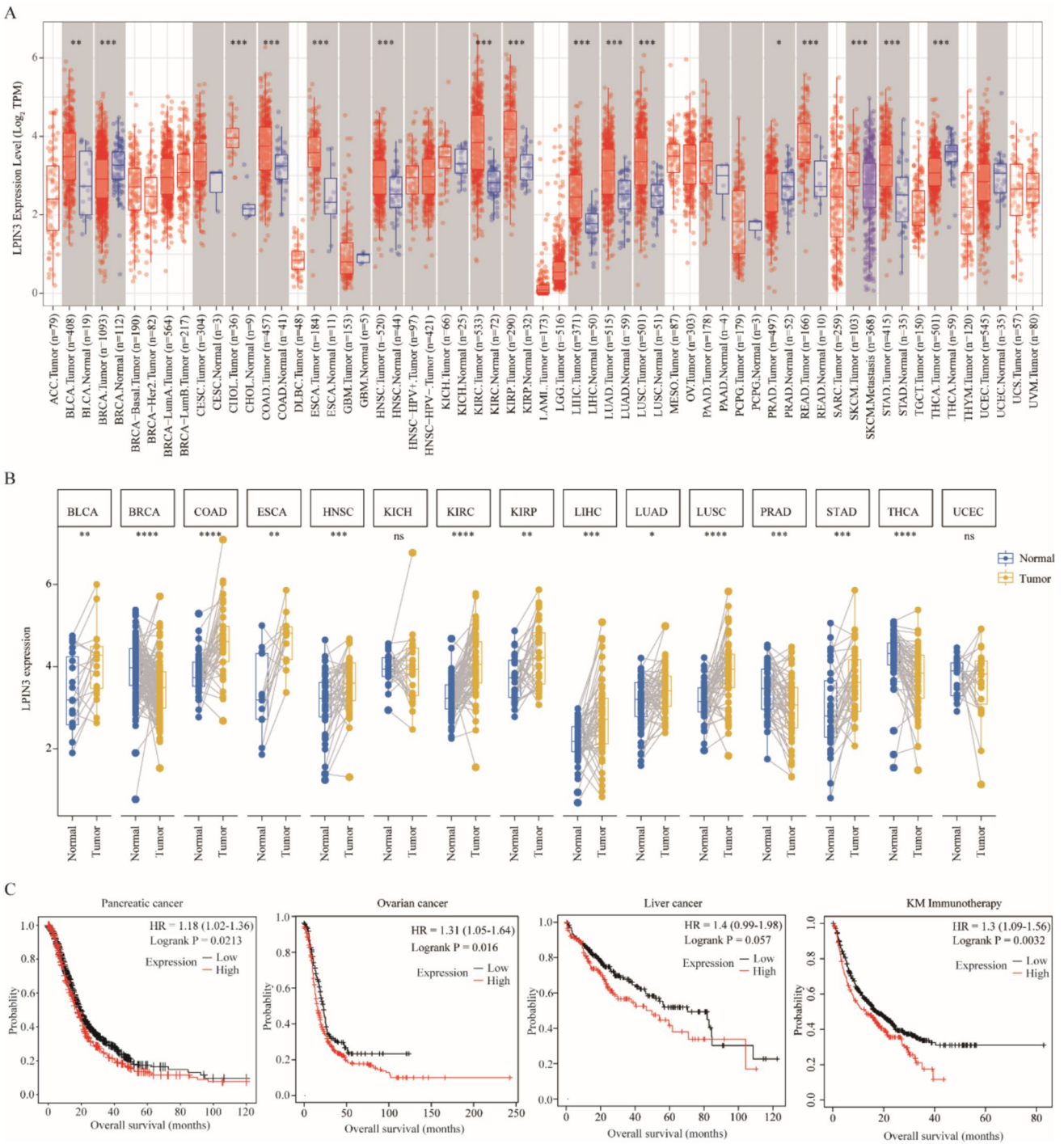

Fig. 1 Expression pattern and prognosis of LPIN3 in pan-cancer. **A** The differential expression analysis of LPIN3 between tumor and normal tissues in 33 cancers. **B** The paired differential expression analysis of LPIN3 in cancers. **C** Kaplan–Meier curves of three cancers and immunotherapy prediction based on the expression of LPIN3

I). However, wild-type LPIN3 rescue significantly rescued the cell proliferation inhibition mediated by LPIN3 knockdown (Fig. 3H, I). The clone formation experiments have also shown that LPIN3 knockdown inhibits the cancer cell growth (Fig. 3J, K). The promotion of apoptosis in HCT116 cells by LPIN3 knockdown was further confirmed by apoptosis tests (Fig. 3L, M).

We also tested the effect of LPIN3 on colorectal cancer cell migration and invasion. The results of scratch assay showed that knockdown of LPIN3 significantly reduced

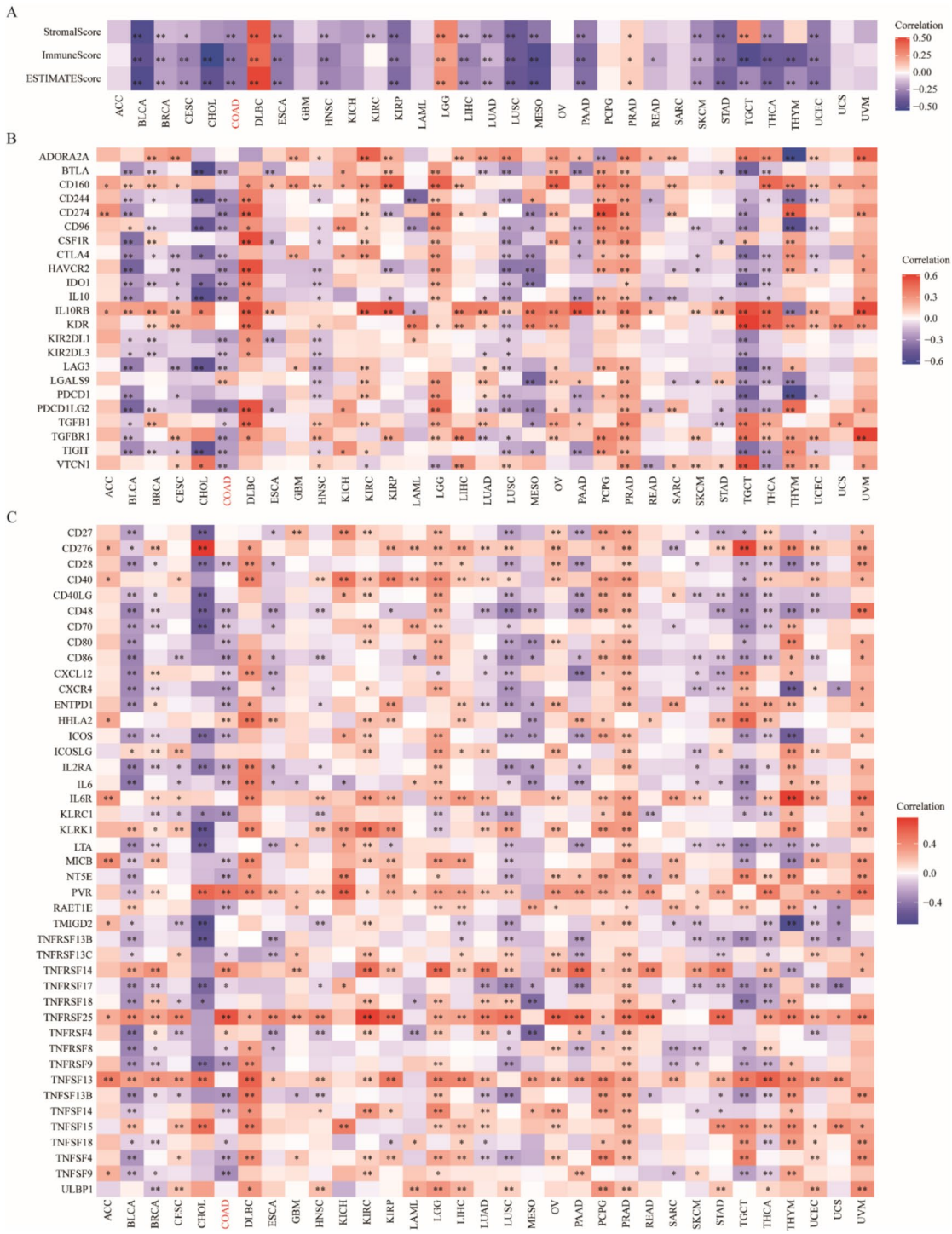

Fig. 2 Tumor immune infiltration, immune-related molecules analysis in pan-cancers based on the expression of LPIN3. **A** Correlation between LPIN3 gene expression and stromal score, immune score, and estimate score. **B** Correlation between LPIN3 gene expression and immune inhibitory molecules. **C** Correlation between LPIN3 gene expression and immune immunostimulatory molecules

the migration of cancer cells (Figure S3A–D). Transwell assay showed that knockdown of LPIN3 significantly reduced the invasion of cancer cells (Figure S3E, F). We then also examined the effect of overexpression of LPIN3 on the phenotype of cancer cells. Cloning assay showed that overexpression of LPIN3 promoted cell proliferation (Figure S3G, H), and similar results were obtained in CCK-8 assay (Figure S3I). The in vivo trial also showed

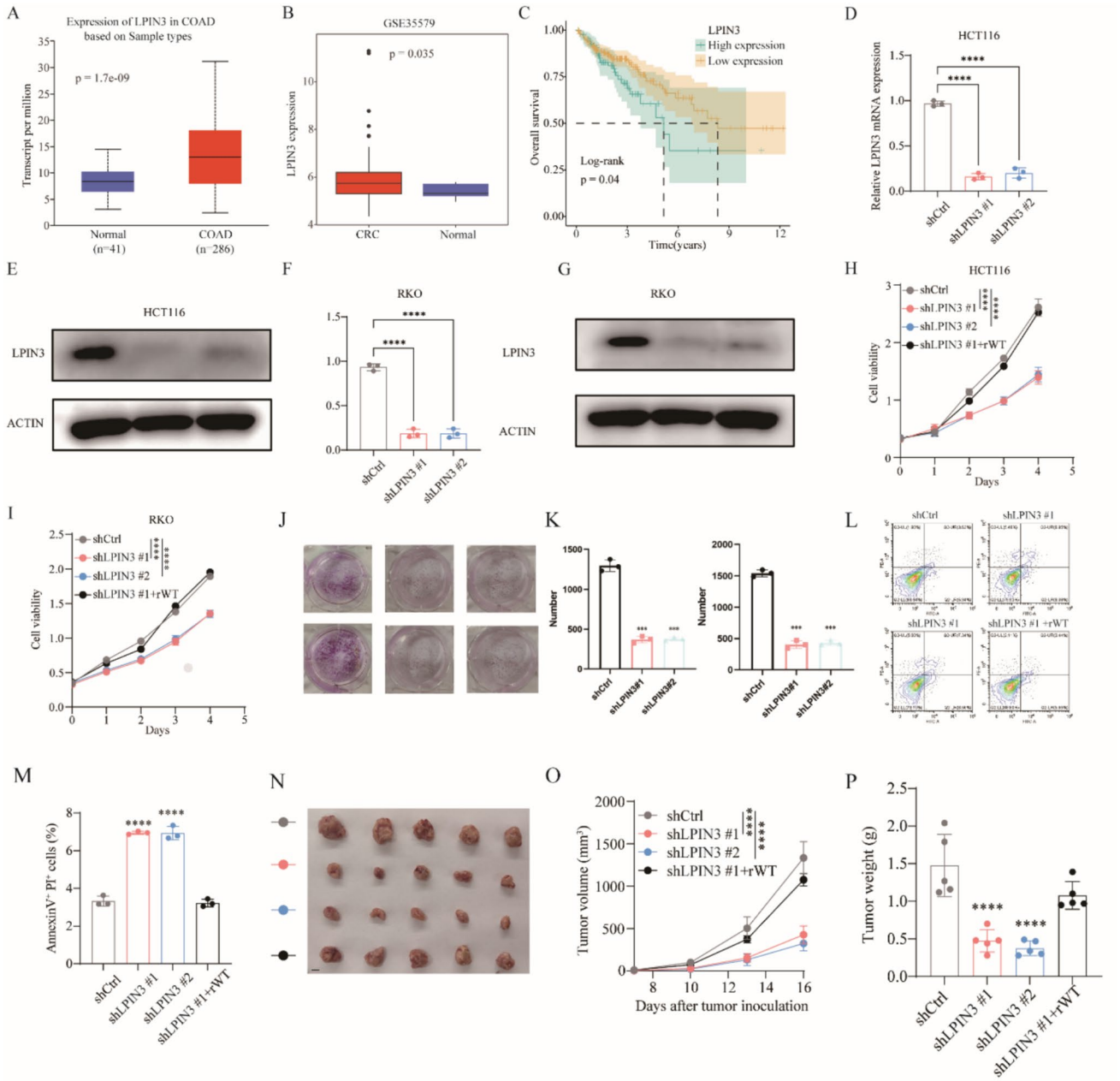

Fig. 3 LPIN3 promotes CRC growth in vivo and in vitro. **A** LPIN3 gene expression level was upregulated in TCGA-COAD datasets. **B** LPIN3 gene expression level was upregulated in GSE35579 datasets. **C** LPIN3 expression and corresponding survival analysis. **D** Relative LPIN3 mRNA level was detected by qPCR in HCT116 cells. **E** Relative LPIN3 protein level was detected by western blot in HCT116 cells. **F** Relative LPIN3 mRNA level was detected by qPCR in RKO cells. **G** Relative LPIN3 protein level was detected by western blot in RKO cells. **H** Effect of LPIN3 on the proliferation of HCT116 cells was assessed using a CCK-8 assay. **I** Effect of LPIN3 on the proliferation of RKO cells was assessed using a CCK-8 assay. **J** Focus formation by HCT116 (up) and RKO (down) cells stably expressing the indicated vectors. **K** Colony numbers of HCT116 (left) and RKO (right) cells are shown in the bar graphs. **L** Cell apoptosis was detected after LPIN3 knockdown. **M** Statistical graph of apoptosis experiments after LPIN3 knockdown. Subcutaneous tumorigenesis in 8 week-old mice: 1×10^6 LPIN3-knockdown or control HCT116 cells were implanted into the mice. **N** tumor image, **O** tumor volume, and **P** tumor weight in mice were shown

that the knockdown of LPIN3 suppressed tumor growth volume and weight (Fig. 3N–P). These findings imply that LPIN3 is involved in the initiation and progression of CRC.

LPIN3 promotes CRC growth through activating β-catenin pathway

Mutational activation of the APC/WNT/β-catenin signaling is pivotal during CRC development [20]; therefore, we

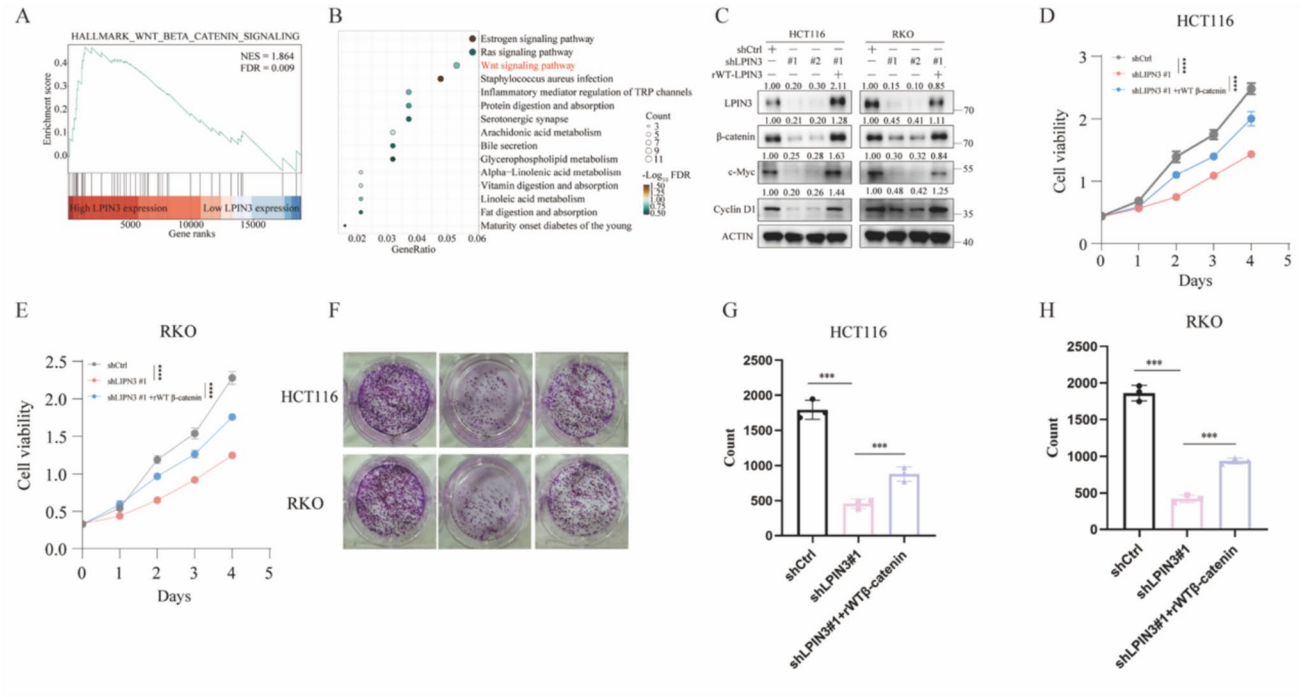

Fig. 4 LPIN3 promotes CRC growth through activating β-catenin pathway. **A** KEGG analysis of upregulated genes based on LPIN3-high versus LPIN3-low patients. **B** GSEA analysis shows that the β-catenin signaling was positive with high LPIN3 expression. **C** The protein expression levels of β-catenin signaling pathway were analyzed by western blotting. **D** Cell proliferation assays of indicated treatment in HCT116 cells. **E** Cell proliferation assays of indicated treatment in RKO cells. **F** Focus formation by HCT116 (up) and RKO (down) cells stably expressing the indicated vectors. **G** Colony numbers of HCT116 cells are shown in the bar graphs. **H** Colony numbers of HCT116 cells are shown in the bar graphs

focused on this signaling pathway. GSEA analysis showed a strong and positive correlation between LPIN3 expression and the Wnt-β-catenin signaling pathway with the TCGA-COAD data (Fig. 4A). The Wnt-β-catenin signaling pathway was also found to be considerably enriched in the LPIN3 high expression group by performing the differential expression and KEGG signaling pathway analysis with the TCGA-COAD data (Fig. 4B). In order to confirm this discovery, we knocked down the expression of LPIN3 in HCT116 and RKO cells. The results showed that LPIN3 suppression markedly decreased Wnt-β-catenin signaling activity as well as the protein levels of downstream target genes c-Myc and Cyclin D1 (Fig. 4C). Similarly, overexpression of LPIN3 significantly promoted this signaling pathway (Figure S3J). We also rescued the β-catenin protein in the shLPIN3 HCT116 and RKO cells for cell proliferation assay, and result showed that rescuing β-catenin expression rescued the cell growth disadvantage caused by LPIN3 knockdown, which indicated that LPIN3 may promote the proliferation of colorectal cancer through the activation of β-catenin signaling (Fig. 4D, E). The clone formation experiments have also shown that rescuing β-catenin expression partly rescued the cancer cell growth (Fig. 4F–H). These findings showed that LPIN3 may stimulate β-catenin signaling, which may contribute to the growth of CRC.

LPIN3 inhibits tumor antigen presentation and the CD8$^+$ T cell killing signals

The major histocompatibility class I (MHC-I) functions as the antigen presentation refers to the "eating me" signaling, which was get scanned by T cell receptors (TCR) and recognized by CD8$^+$ T lymphocytes thereby destroying tumor cells. Consequently, we examined the relationship between the expression of LPIN3 and tumor mutational load (TMB) and microsatellite instability (MSI) with the TCGA-COAD data. TMB and MSI, at least in COAD, demonstrated a negative connection with one another (Figure S4A). After that, we also found that those genes that down-regulated in the high LPIN3 expression patients were enriched in the antigen processing and presentation by the KEGG enrichment with the TCGA-COAD data (Fig. 5A). The GSEA analysis showed that high LPIN3 expression significantly correlated with the decreased antigen processing and presentation signaling and interferon gamma response (Figs. 5B and S4B). The correlation analysis with the TCGA-COAD data suggested that LPIN3 expression was negatively correlated with the several

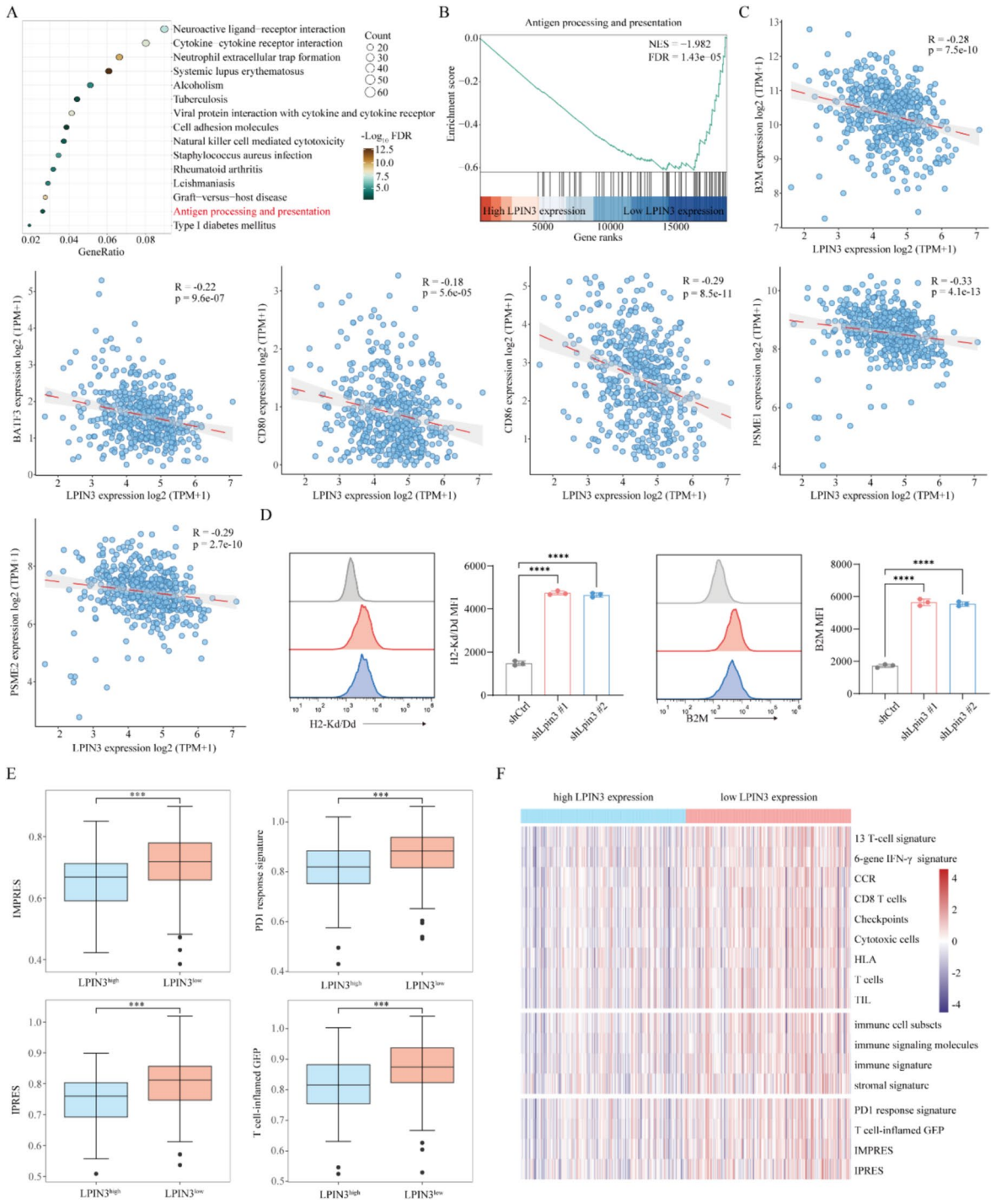

Fig. 5 LPIN3 inhibits tumor antigen presentation and the CD8$^+$ T cell killing signals. **A** KEGG analysis of down-regulated genes based on LPIN3-high versus LPIN3-low patients. **B** GSEA analysis shows that the antigen processing and presentation signaling was positive with high LPIN3 expression. **C** Correlation between LPIN3 gene expression and some antigen processing and presentation-related molecules. **D** LPIN3 knockdown increased tumor antigen presentation. **E** Heatmap map showed LPIN3 gene expression and several T cell-related signaling. **F** Several immune responsive signaling-based LPIN3 gene expression

MHC-I molecules such as B2M, BATF3 et al. (Fig. 5C). To further validate these biological phenomenon, we knocked down the expression of LPIN3 in CT26 tumor cell line to examine the expression of MHC-I molecules. The results revealed that knockdown of LPIN3 significantly upregulated the expression of H2-Kb/Dd and B2M molecules (Fig. 5D). It

indicates that LPIN3 inhibition significantly enhances antigen presentation in CRC tumors. Furthermore, higher enrichment scores of T cell inflamed gene expression profile (GEP), innate anti-PD-1 resistance (IPRES), PD-1 response signature, and immuno-predictive score (IMPRES) signatures were observed in LPIN3-high samples compared with LPIN3-low samples (Fig. 5E). LPIN3-low patients exhibited significant enrichment of signatures identifying $CD8^+$ T cell effector function signal or immune response (Fig. 5F). Meanwhile, ssGSEA analysis in the TCGA-COAD dataset showed that samples with

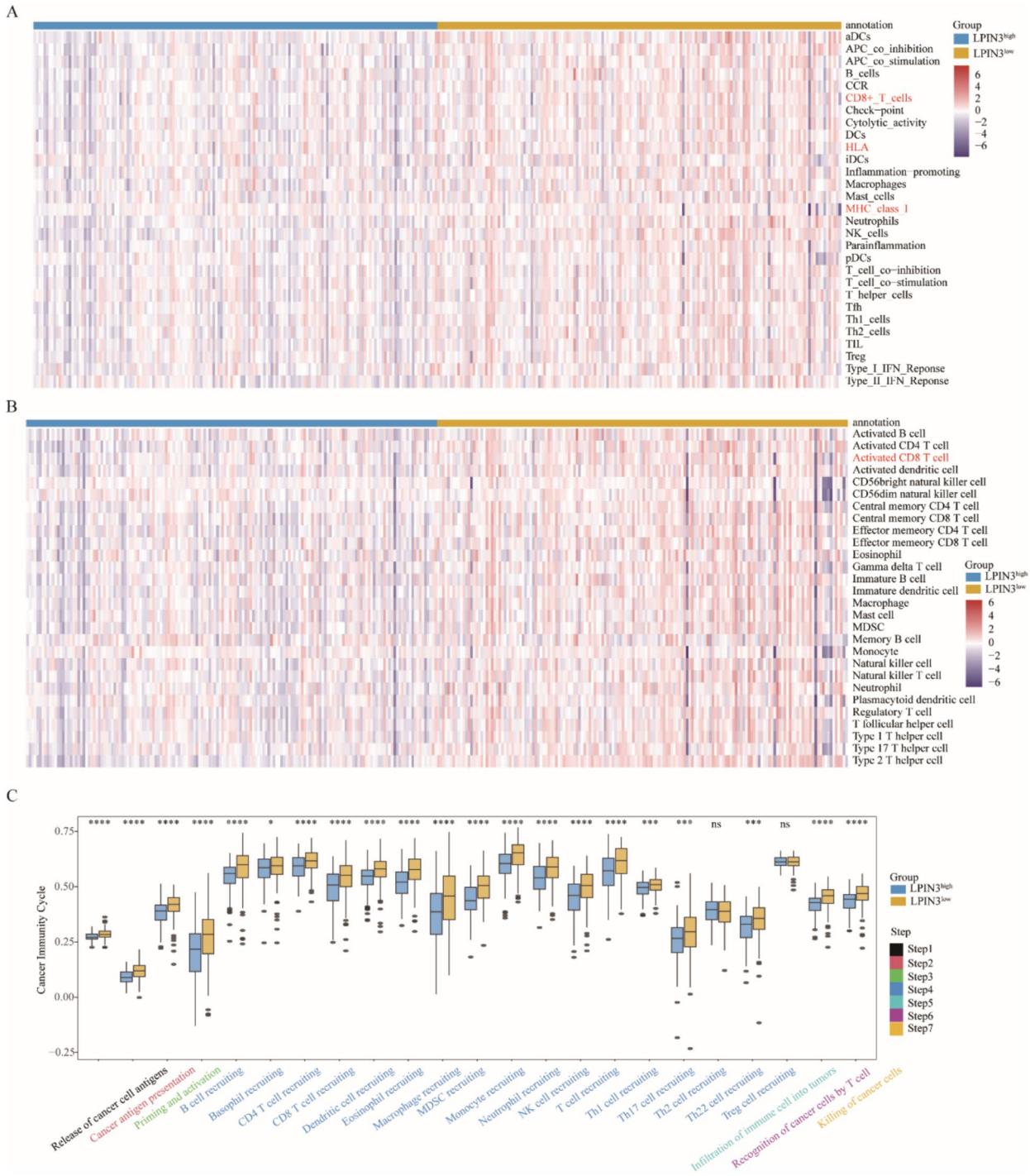

Fig. 6 LPIN3 inhibits T cell-related effect signal. **A** Heatmap showed immune-related signaling between high and low LPIN3 expression in TCGA-COAD dataset. **B** Heatmap showed immune cell infiltration between high and low LPIN3 expression in TCGA-COAD dataset. **C** The steps of the cancer-immunity cycle score were calculated by ssGSEA algorithms

low LPIN3 expression had higher levels of signals, including $CD8^+$ T cell infiltration, HLA molecules, and interferon response (Fig. 6A). And patients with decreased expression of LPIN3 had higher levels of immune cell infiltration, including activated $CD8^+$ T cells (Fig. 6B). We also calculated the cancer-immunity cycle and the tumor microenvironment scores, which showed tumor samples with low LPIN3 expression had higher tumor immunity-related scores (Fig. 6C). Taken together, these data indicate that LPIN3 could inhibit MHC-I presentation and $CD8^+$ T cell effector function signal.

LPIN3 inhibition suppresses tumor growth by promoting $CD8^+$ T cell infiltration

Our further analysis revealed that the expression of LPIN3 was significantly negatively correlated with the expression of several effector molecules of $CD8^+$ T cells (Figures S4C and S5), suggesting that LPIN3 may inhibit the effector function of $CD8^+$ T cells in tumors. To investigate the role of LPIN3 in tumor immune evasion, we knocked down LPIN3 in CT26 cells (Fig. 7A). Because it has been previously reported in the literature that the β-catenin/TCF/LEF complex to the promoter region of the CD274 gene induces PD-L1 expression [21], we then speculated whether LPIN3 could promote PD-L1 expression. Western blot showed that knockdown of LPIN3 also significantly reduced PD-L1 expression (Fig. 7A), and the reduced PD-L1 expression may be associated with T cell activation. Flow cytometry also showed that knockdown of LPIN3 also significantly reduced PD-L1 expression (Fig. 7B, C). In subcutaneous tumorigenic experiment, the results showed that knockdown of LPIN3 significantly decreased tumor volume and tumor weight (Fig. 7D–F). Flow cytometric analysis of the aforementioned tumor tissues revealed that knockdown of LPIN3 could significantly promote the $CD8^+$ T cell infiltration (Fig. 7G, H). The T cell exhaustion marker PD-1 and TOX was also examined by flow cytometry, displaying that knockdown of LPIN3 decreased these molecules expression (Figs. 7I, J, 8A, B). Flow cytometry was further used to analyze the role of LPIN3 in cytokines secreted by $CD8^+$ T cells. It was found that the knockdown of LPIN3 in CT26 cells markedly increased the abundance of IFN-γ, TNF-α, and IL-2 secreted by $CD8^+$ T cells (Fig. 8C–H). Taken together, these results revealed that LPIN3 inhibition may promote $CD8^+$ T cell infiltration and effect function in CRC mouse model.

Discussion

Immunotherapy is one of the most important therapeutic methods for cancers, especially the anti-PD-1 or anti-PD-L1 treatment. Revolutionary progress in anti-PD-1 treatment brings the curative hope of metastatic colorectal cancer [22, 23]. However, due to tumor heterogeneity, the potent of anti-PD-1 treatment in proficient mismatch repair (pMMR) CRC is still limited. Specifically, the abundance of $CD8^+$T cells in cancers almost determines the efficacy of immunotherapy. Studies demonstrated that the level of $CD8^+$T cell infiltration in deficient mismatch repair (dMMR) is much higher than that in pMMR CRC [24]. Therefore, strategies that improve the $CD8^+$T cell infiltration may be the pivotal treatment approaches for CRC. In the present study, we found that LPIN3 was highly expressed in BLCA, KIRC, HNSC, LIHC, LUAD, LUSC, STAD, and COAD through differential expression analysis in pan-cancers. KM analysis showed that high expression of LPIN3 was associated with a worse prognosis in CRC, pancreatic adenocarcinoma, breast carcinoma and LIHC. These results suggested that LPIN3 may play a significant role in tumor progression. To this end, we constructed the LPIN3 inhibition CRC cells, the knockdown of LPIN3 inhibited the proliferation of CRC cell lines, which was proved in xenograft experiments. Meanwhile, inhibition of LPIN3 in CRC cells promoted apoptosis. To our knowledge, the role of LPIN3 was merely reported in the lipid metabolism [9]. Therefore, our results may provide a novel target for CRC treatment.

To disclose the underlying mechanism of LPIN3 in CRC, we performed the KEEG pathway analysis, indicating that high LPIN3 expression is mainly enriched in the Wnt/β-catenin signaling pathway. Subsequent experiments confirmed that LPIN3 contributed to the proliferation of CRC and may activate the Wnt/β-catenin signaling pathway. The Wnt/β-catenin signaling pathway also named the canonical Wnt signaling pathway played a pivotal role in the apoptosis, proliferation, and metabolism of CRC [25]. To date, small molecular inhibitors or phytochemicals for the Wnt pathway of CRC treatment have been developed, such as Pimozide and DK419 [26]. Therefore, our results may contribute to the regulation of the Wnt/β-catenin signaling pathway, providing a new target for combination therapy of CRC.

Additionally, we discovered that LPIN3 is playing an increasingly important role in tumor immune evasion, emphasizing its roles in immune checkpoint control, immune cell recruitment, and tumor microenvironment metabolic reprogramming. An analysis of the relationship between LPIN3 expression and immune system activation in colon cancer tissues revealed a negative correlation between LPIN3 expression and tumor antigen presentation, $CD8^+$ T cell infiltration, and the expression of T cell effector molecules like IFN-γ and GAMB. We also used flow cytometry to confirm these intriguing results. IFN-γ that mediates the antitumor immunity is mainly secreted by $CD8^+$ T cells in cancers [27]. Cancer cells could adopt strategies such as inhibiting the $CD8^+$ T cell tumor trafficking, survival, and function to decrease the secretion of IFN-γ [28]. On the

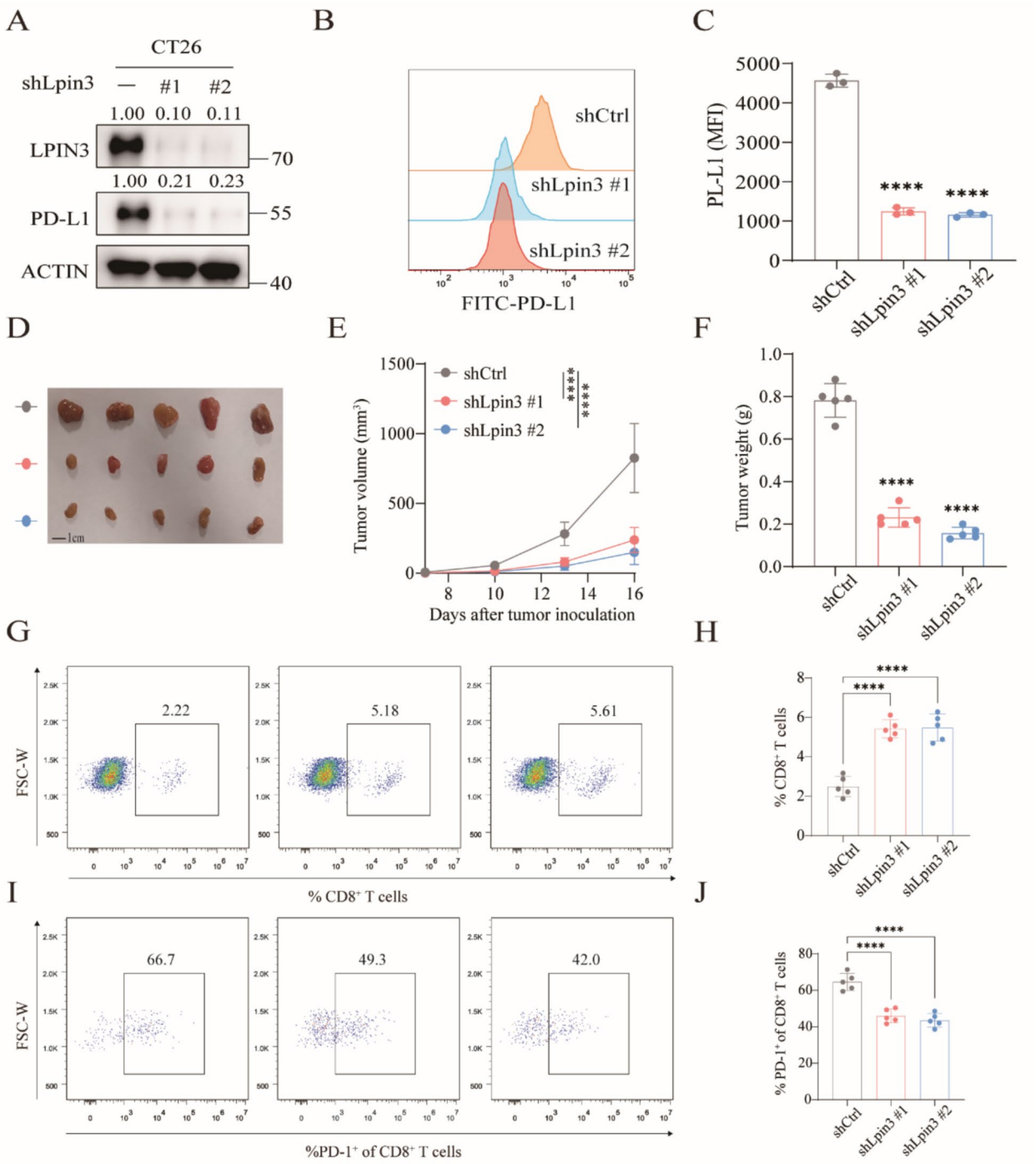

Fig. 7 LPIN3 inhibition suppresses tumor growth by promoting $CD8^+$ T cell infiltration. **A** PD-L1 abundance was detected by Western bolt based on LPIN3 knockdown. **B** PD-L1 abundance was detected by flow cytometry based on LPIN3 knockdown. **C** Statistical graph of **B** experiments. Subcutaneous tumorigenesis in 8-week-old mice: 1×10^6 LPIN3-knockdown or control CT26 cells were implanted into the mice. Detection of tumor image (**D**), tumor volume (**E**) and tumor weight (**F**) in mice. **G** Representative flow staining of $CD8^+$ T cells frequency in the indicated groups. **H** Statistical graph of **G** experiments. **I** Representative flow staining of PD-1^+ $CD8^+$ T cells frequency in the indicated groups. **J** Statistical graph of **I** experiments

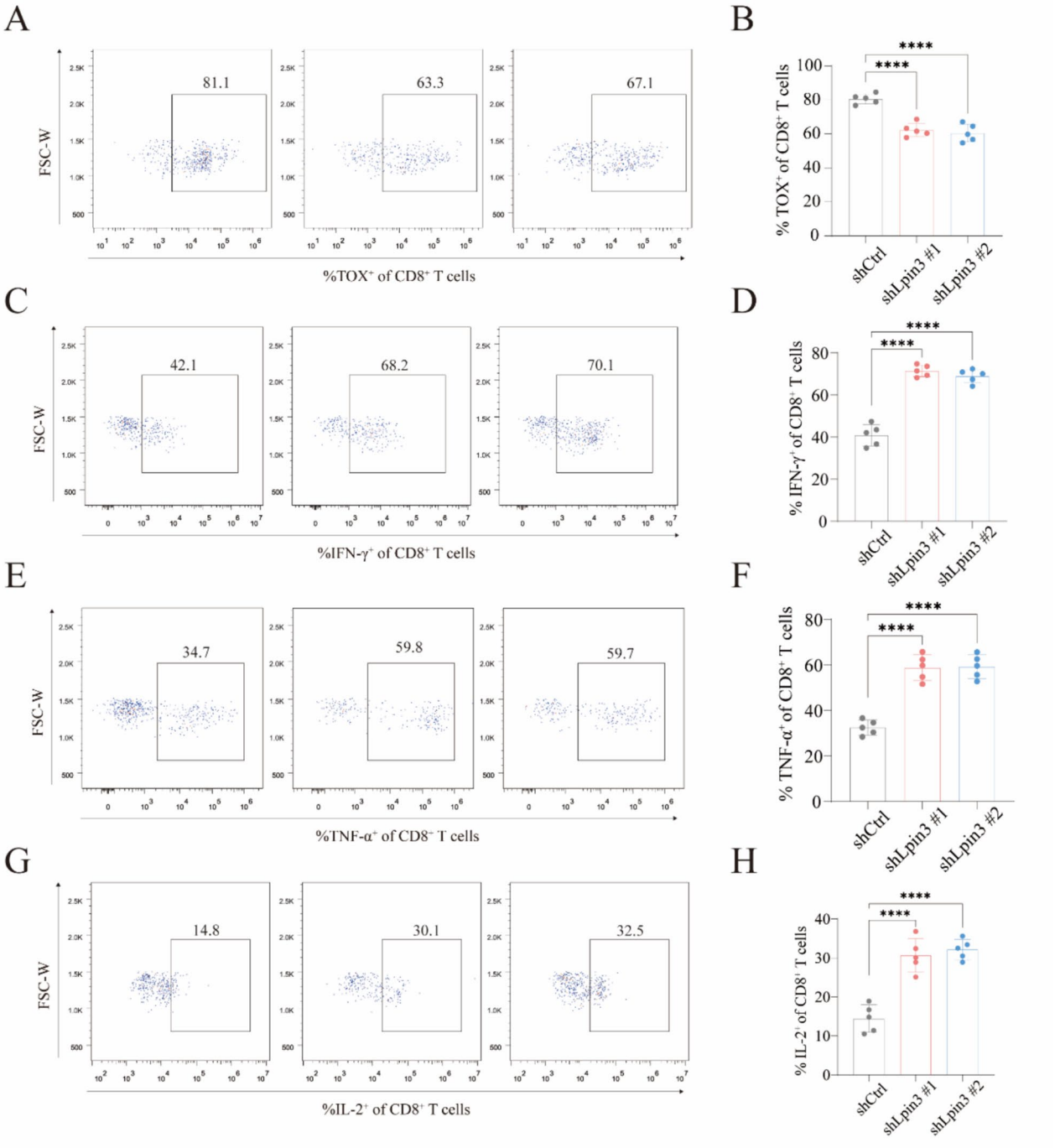

Fig. 8 LPIN3 inhibition enhancing tumor-infiltrating $CD8^+$ T cell function. **A** Representative TOX^+ $CD8^+$ T flow staining of indicated cells in tumor xenograft of indicated groups. **B** Statistical graph of **A** experiments. **C** Representative IFN-γ^+ $CD8^+$ T flow staining and frequency of indicated cells in tumor xenograft of indicated groups. **D** Statistical graph of **C** experiments. **E** Representative TNF-α^+ $CD8^+$ T flow staining and frequency of indicated cells in tumor xenograft of indicated groups. **F** Statistical graph of **E** experiments. **G** Representative IL-2^+ $CD8^+$ T flow staining and frequency of indicated cells in tumor xenograft of indicated groups. **H** Statistical graph of **G** experiments

contrary, strategies that are applied to tumor treatments aim to activate the $CD8^+$ T cell thereby promoting the secretion of IFN-γ. For example, the downregulation of ER stress sensor X-box binding protein 1 decreased the metabolism in $CD8^+$ T cells, thus restoring the antitumor activity [29]. To this end, we can make the TME more inclined to promote the secretion of IFN-γ. In our study, we inhibited the expression of LPIN3 and observed that LPIN3 inhibition impeded the tumor growth and markedly promoted the proportion of IFN-γ + /CD8 + T cells in the tumor microenvironment in a subcutaneous transplantation model of colon cancer in mice. The results of the experiment match those of the TCGA correlation study, indicating that LPIN3 suppresses the T cell-mediated tumor immune response, thereby promoting the progression of colon cancer. On the other hand, MHC-I complex could regulate the antitumor immunity due to the antigens presentation [30]. Similarly, cancers avoided immune surveillance by downregulating the expression of the MHC- I complex, such as B2M, the light chain of the MHC- I complex [31]. And strategies that promoted the expression of B2M also enhanced the antitumor activity [32]. In our study, we observed and validated that LPIN3 was negatively associated with B2M, highlighting the role of LPIN3 inhibition in the antitumor activity.

In conclusion, the present study's findings indicate that LPIN3 can stimulate the β-catenin signaling pathway, which in turn can increase colon cancer immune evasion. Additionally, it can block $CD8^+$ T cells by suppressing tumor antigen presentation. Therefore, our research offers a mechanistic understanding as well as a possible therapeutic approach, namely that targeting LPIN3 may improve the effectiveness of anti-PD-1 in the treatment of human malignancies.

Supplementary Information The online version contains supplementary material available at https://doi.org/10.1007/s00262-025-03989-2.

Author contributions Conceptualization was done by C.J., H.W., and Y.S.; methodology, software, formal analysis, and data curation were done by X.Z., H.F., and Y.S.; validation was done by X.Z., H.F., and W.W.; writing—original draft preparation was done by X.Z., H.F., and Y.S.; writing—review and editing was done by X.Z., H.F., C.J., and Y.S. All authors have read and agreed to the published version of the manuscript.

Funding This study was supported by the National Natural Science Foundation of China (Grant Number: 82303181).

Availability of data and materials No datasets were generated or analyzed during the current study.

Declarations

Conflict of interest The authors declare no competing interests.

Ethics approval The animal experimentation was approved by the Experimental Animal Welfare Ethics Committee, Zhongnan Hospital of Wuhan University (ZN2024117).

References

1. Li JX, Ma XD, Chakravarti D, Shalapour S, DePinho RA (2021) Genetic and biological hallmarks of colorectal cancer. Gene Dev 35(11–12):787–820. https://doi.org/10.1101/gad.348226.120
2. Han B, Zheng R, Zeng H, Wang S, Sun K, Chen R et al (2024) Cancer incidence and mortality in China, 2022. J Natl Cancer Center 4(1):47–53. https://doi.org/10.1016/j.jncc.2024.01.006
3. Michot C, Hubert L, Romero NB, Gouda A, Mamoune A, Mathew S et al (2012) Study of LPIN1, LPIN2 and LPIN3 in rhabdomyolysis and exercise-induced myalgia. J Inherit Metab Dis 35(6):1119–1128. https://doi.org/10.1007/s10545-012-9461-6
4. He XP, Xu XW, Liu B (2009) Molecular characterization, chromosomal localization and association analysis with back-fat thickness of porcine LPIN2 and LPIN3. Mol Biol Rep 36(7):1819–1824. https://doi.org/10.1007/s11033-008-9385-2
5. Zhang P, Csaki LS, Ronquillo E, Baufeld LJ, Lin JY, Gutierrez A et al (2019) Lipin 2/3 phosphatidic acid phosphatases maintain phospholipid homeostasis to regulate chylomicron synthesis. J Clin Invest 129(1):281–295. https://doi.org/10.1172/JCI122595
6. Ingram LM, Finnerty MC, Mansoura M, Chou CW, Cummings BS (2021) Identification of lipidomic profiles associated with drug-resistant prostate cancer cells. Lipids Health Dis 20(1):ARTN 15. https://doi.org/10.1186/s12944-021-01437-5
7. Zhang ZH, Huang YQ, Li S, Hong L (2024) Comprehensive analysis based on glycolytic and glutaminolytic pathways signature for predicting prognosis and immunotherapy in ovarian cancer. J Cancer 15(2):383–400. https://doi.org/10.7150/jca.88359
8. Liu JH, Xu W, Li SY, Sun R, Cheng WJ (2020) Multi-omics analysis of tumor mutational burden combined with prognostic assessment in epithelial ovarian cancer based on TCGA database. Int J Med Sci 17(18):3200–3213. https://doi.org/10.7150/ijms.50491
9. Meidtner K, Fisher E, Ängquist L, Holst C, Vimaleswaran KS, Boer JMA et al (2014) Variation in genes related to hepatic lipid metabolism and changes in waist circumference and body weight. Genes Nutr. https://doi.org/10.1007/s12263-014-0385-7
10. He X, Xu C (2020) Immune checkpoint signaling and cancer immunotherapy. Cell Res 30(8):660–669. https://doi.org/10.1038/S51422-020-0343-4
11. Galassi C, Chan TA, Vitale I, Galluzzi L (2024) The hallmarks of cancer immune evasion. Cancer Cell 42(11):1825–1863. https://doi.org/10.1016/j.ccell.2024.09.010
12. Belk JA, Daniel B, Satpathy AT (2022) Epigenetic regulation of T cell exhaustion. Nat Immunol 23(6):848–860. https://doi.org/10.1038/S51590-022-01224-z
13. Ren JL, Li N, Pei SY, Lian YN, Li L, Peng YC et al (2022) Histone methyltransferase WHSC1 loss dampens MHC-I antigen presentation pathway to impair IFN-γ stimulated antitumor immunity.

J Clin Investig 132(8):ARTN e153167. https://doi.org/10.1172/JCI153167
14. Wang X, Chai YY, Quan Y, Wang JM, Song JY, Zhou WK et al (2024) NPM1 inhibits tumoral antigen presentation to promote immune evasion and tumor progression. J Hematol Oncol 17(1):ARTN 97. https://doi.org/10.1186/s13045-024-01618-6
15. Yang ZL, Huo YZ, Zhou SX, Guo JY, Ma XT, Li T et al (2022) Cancer cell-intrinsic XBP1 drives immunosuppressive reprogramming of intratumoral myeloid cells by promoting cholesterol production. Cell Metab 34(12):2018-+. https://doi.org/10.1016/j.cmet.2022.10.010
16. Zhao J, Zhou X, Chen B, Lu M, Wang G, Elumalai N et al (2023) p53 promotes peroxisomal fatty acid beta-oxidation to repress purine biosynthesis and mediate tumor suppression. Cell Death Dis 14(2):87. https://doi.org/10.1038/S51419-023-05625-2
17. Liu Y, Liang GH, Xu HJ, Dong WX, Dong Z, Qiu ZW et al (2021) Tumors exploit FTO-mediated regulation of glycolytic metabolism to evade immune surveillance. Cell Metab 33(6):1221-+. https://doi.org/10.1016/j.cmet.2021.04.001
18. Pan Y, Chen H, Zhang X, Liu W, Ding Y, Huang D et al (2023) METTL3 drives NAFLD-related hepatocellular carcinoma and is a therapeutic target for boosting immunotherapy. Cell Rep Med. https://doi.org/10.1016/j.xcrm.2023.101144
19. Hänzelmann S, Castelo R, Guinney J (2013) GSVA: gene set variation analysis for microarray and RNA-Seq data. BMC Bioinform. https://doi.org/10.1186/1471-2105-14-7
20. Peuker K, Muff S, Wang J, Kunzel S, Bosse E, Zeissig Y et al (2016) Epithelial calcineurin controls microbiota-dependent intestinal tumor development. Nat Med 22(5):506–515. https://doi.org/10.1038/nm.4072
21. Du L, Lee J-H, Jiang H, Wang C, Wang S, Zheng Z et al (2020) β-Catenin induces transcriptional expression of PD-L1 to promote glioblastoma immune evasion. J Exp Med. https://doi.org/10.1084/jem.20191115
22. André T, Shiu K-K, Kim TW, Jensen BV, Jensen LH, Punt C et al (2020) Pembrolizumab in microsatellite-instability–high advanced colorectal cancer. N Engl J Med 383(23):2207–2218. https://doi.org/10.1056/NEJMoa2017699
23. Hu Y, Liu L, Jiang Q, Fang W, Chen Y, Hong Y et al (2023) CRISPR/Cas9: a powerful tool in colorectal cancer research. J Exp Clin Cancer Res. https://doi.org/10.1186/s13046-023-02901-z
24. Amodio V, Lamba S, Chilà R, Cattaneo CM, Mussolin B, Corti G et al (2023) Genetic and pharmacological modulation of DNA mismatch repair heterogeneous tumors promotes immune surveillance. Cancer Cell 41(1):196-209.e5. https://doi.org/10.1016/j.ccell.2022.12.003
25. Zhang Y, Wang X (2020) Targeting the Wnt/β-catenin signaling pathway in cancer. J Hematol Oncol. https://doi.org/10.1186/s13045-020-00990-3
26. Zhao H, Ming T, Tang S, Ren S, Yang H, Liu M et al (2022) Wnt signaling in colorectal cancer: pathogenic role and therapeutic target. Mol Cancer 21(1):144. https://doi.org/10.1186/s12943-022-01616-7
27. Du W, Frankel TL, Green M, Zou W (2022) IFNγ signaling integrity in colorectal cancer immunity and immunotherapy. Cell Mol Immunol 19(1):23–32. https://doi.org/10.1038/S51423-021-00735-3
28. Pitt JM, Vetizou M, Daillere R, Roberti MP, Yamazaki T, Routy B et al (2016) Resistance mechanisms to immune-checkpoint blockade in cancer: tumor-intrinsic and -extrinsic factors. Immunity 44(6):1255–1269. https://doi.org/10.1016/j.immuni.2016.06.001
29. Ma XZ, Bi EG, Lu Y, Su P, Huang CJ, Liu LT et al (2019) Cholesterol induces CD8 T cell exhaustion in the tumor microenvironment. Cell Metab 30(1):143-+. https://doi.org/10.1016/j.cmet.2019.04.002
30. Wu X, Li T, Jiang R, Yang X, Guo H, Yang R (2023) Targeting MHC-I molecules for cancer: function, mechanism, and therapeutic prospects. Mol Cancer. https://doi.org/10.1186/s12943-023-01899-4
31. Blees A, Januliene D, Hofmann T, Koller N, Schmidt C, Trowitzsch S et al (2017) Structure of the human MHC-I peptide-loading complex. Nature 551(7681):525–528. https://doi.org/10.1038/nature24627
32. Wang H, Liu B, Wei J (2021) Beta2-microglobulin(B2M) in cancer immunotherapies: Biological function, resistance and remedy. Cancer Lett 517:96–104. https://doi.org/10.1016/j.canlet.2021.06.008